# Synthesis, Characterization, Thermal Study, Biological Activity and Corrosion Inhibition of New Ligand Derived from Butanedioyl Dichloride and Some Selective Transition Metal Compl…

**Article** · February 2019

CITATIONS
0

READS
16

**2 authors**, including:

Enass Jasim Waheed
University of Baghdad
**19** PUBLICATIONS **15** CITATIONS

SEE PROFILE

ISSN: 0975 -8542

Journal of Global Pharma Technology

Available Online at: www.jgpt.co.in

RESEARCH ARTICLE

# Synthesis, Characterization, Thermal Study, Biological Activity and Corrosion Inhibition of New Ligand Derived from Butanedioyl Dichloride and Some Selective Transition Metal Complexes

**Enass J. Waheed[1*], Awf A.R. Ahmed[2]**

1. *Department of Chemistry, College of Education for Pure Sciences, Ibn -Al-Haitham, University of Baghdad, Adhamiyah, Baghdad, Iraq.*

2. *Ministry of Education/Directorate of Education Rusafa first, Iraq.*

***Corresponding Author: Enass J. Waheed**

## Abstract

The new ligand [N1,N4-bis((1H-benzo[d]Glyoxalin-2-yl)carbamothioyl)Butanedi amide] (NCB) derived from Butanedioyl diisothiocyanate with 2-aminobenz imidazole was used to prepare a chain of new metal complexes of Cr(III), Mn(II), Co(II), Ni(II), Cu(II), Pd(II), Ag(I), Cd(II) by general formula [M(NCB)]Xn ,Where M= Cr(III), n=3, X=Cl; Mn(II), Co(II), Ni(II), Cu(II), Pd(II), Cd(II) ,n=2 , X=Cl; Ag(I), n=1, X=$NO_3$. Characterized compounds on the basis of $^1$H, $^{13}$CNMR (for (NCB), FT-IR and U.V spectrum, melting point, molar conduct, %C, %H, %N and %S, the percentage of the metal in complexes %M, Magnetic susceptibility, thermal studies (TGA),while its corrosion inhibition for mild steel in $Ca(OH)_2$ solution is studied by weight loss. These measurements indicate that (NCB) coordinates with the metal ion in a hexadentate manner through the sulfur and nitrogen atoms and the octahedral structure of these complexes is suggested. The anti-bacterial activity of the complexes against two types of bacterial *Staphylococcus Aureus* (+) and *Escherichia Coli* (-) for the metal complexes was higher than for free ligand (NCB).

**Keywords:** *Butanedioyl dichloride, Corrosion inhibition, Biological activity.*

## Introduction

Benzimidazole is a heterocyclic organic aromatic compound. It comes back to bicyclic ring system and has different pharmacological uses. Among the heterocyclic derivatives, Because of the unique structure of diagnostic and therapeutic factors, 2-aminobenzimidazole has become more interesting [1, 2]. 2-Aminobenzimidazole (ABI) have diverse applications in coordination chemistry, photo physics, photochemistry, bioinorganic chemistry ,biological activities include anti-cancer, bactericidal, fungicidal, analgesic, viral ,pharmacokinetic and pharmacodynamics properties.

Specifically, this nucleus is a constituent of vitamin $B_{12}$. Also, Because of anti-histamine activity, local analgesic, inhibition of cells, hypokalemia and inflammation of the ligand increased its importance [3, 4]. Transition metal complexes containing (ABI) are widely used as catalysts for hydrogenation, hydroformylation, oxidation and other reactions. Because of the promising therapeutic potential of benzimidazole complexes have begun to be used to model important biological systems; most of the works carried out on these types of compound are related to their medical features. The N and S hetero atoms play an essential role in the coordination of metals at the active sites of various metallobiomolecule and viewed as promising pharmaceutical agents with antioxidant/free radical scavenging properties [5, 6]. (ABI) have been used as corrosion inhibitors for copper, zinc, steel and brass in different environments.

The inhibition performance of (ABI) as corrosion inhibitors in (acid or base) media mild steel corrosions, using molecular dynamic simulation and quantum chemistry calculations, we evaluated the theoretical and analysis steps to inhibition corrosion [7, 8].

The aim of the current study to define the structure and geometry of the ligand (NCB) and its complexes to ions Cr(iii), Mn(ii), Co(ii), Ni(ii), Cu(ii), Pd(ii), Ag(i), Cd(ii).

## Experimental Section

## Materials and Methods

From commercial sources we obtained all chemical and analytical reagents and were used without further purification. From (the United States of America, Sigma - Aldrich, Merck and India) various chemicals, metal salts and solvents used in this research were purchased. The melting point of the synthesized compounds was determined in an open capillary tube with an electro thermal melting point apparatus (SMP10 Stuart). Using FT-IR test scan Shimadzu (FT-IR) - 8300 series spectro photometer in the range (400-4000) $cm^{-1}$, FT-IR spectra (KBr pellets) have been measured.

Using Shimadzu UV-visible-160 A Ultra Violet-Visible Spectrophotometer with a quartz cell length of 1.0 cm and a concentration of $10^{-3}$ M from the samples in the DMSO solvent at room temperature, the electronic spectra of the compound were measured. Through the atomic absorption technique (A.A) by a. Shimadzu (AA 680), the percentage of metals has been determined. Using the Bruker 300 MHz NMR spectrometer, the NMR spectra $^{1}H$ and $^{13}C$ in a dimethyl sulfoxide solution (DMSO-d6 with TMS) have been recorded. Using the Eutech 150 conductivity meter, the conductivity measurements at room temperature and $10^{-3}$M concentration of the sample solution in the DMSO solvent were conducted. By Euro EA 300, Micro elemental analysis for carbon, hydrogen and nitrogen has been determined. With the magnetic sensitivity balance (Sherwood Scientific), magnetic moments (μeff B.M) at 25 ° C have been identified. A STA PT-1000 Linseis at the temperature range of 0-600 ℃ and used argon gas, thermal gravity analysis (TGA) was performed.

## The Organic Compound

### Synthesis of Ligand (NCB) [9]

In dry acetone (20 ml), butanedioyl dichloride (0.929 g, 6 mmol) was dissolved. In dry acetone (15 ml), Sodium thiocyanate (0.486 g, 6 mmol) was dissolved. Slowly to the first solution, the last solution was added and at room temperature for one hour, the reaction mixture was stirred.

The white precipitate of sodium chloride was filtered off. In dry acetone (15 ml), dissolve 2-amino benzimidazole (0.798 g, 6 mmol) was added to the filtrate containing Butanedioyl diisothiocyanate intermediate. For 22-28 hours, the reaction mixture was refluxed. By adding an additional amount of ice powder to the flask the solution has been allowed to cool down. In the form of a precipitate, the NCB was collected and several times with water was washed, above the silica gel has been dried and using DMSO has been re-crystallized to afford ligand (NCB) in good yield (85%, Scheme 1,Fig.(1).

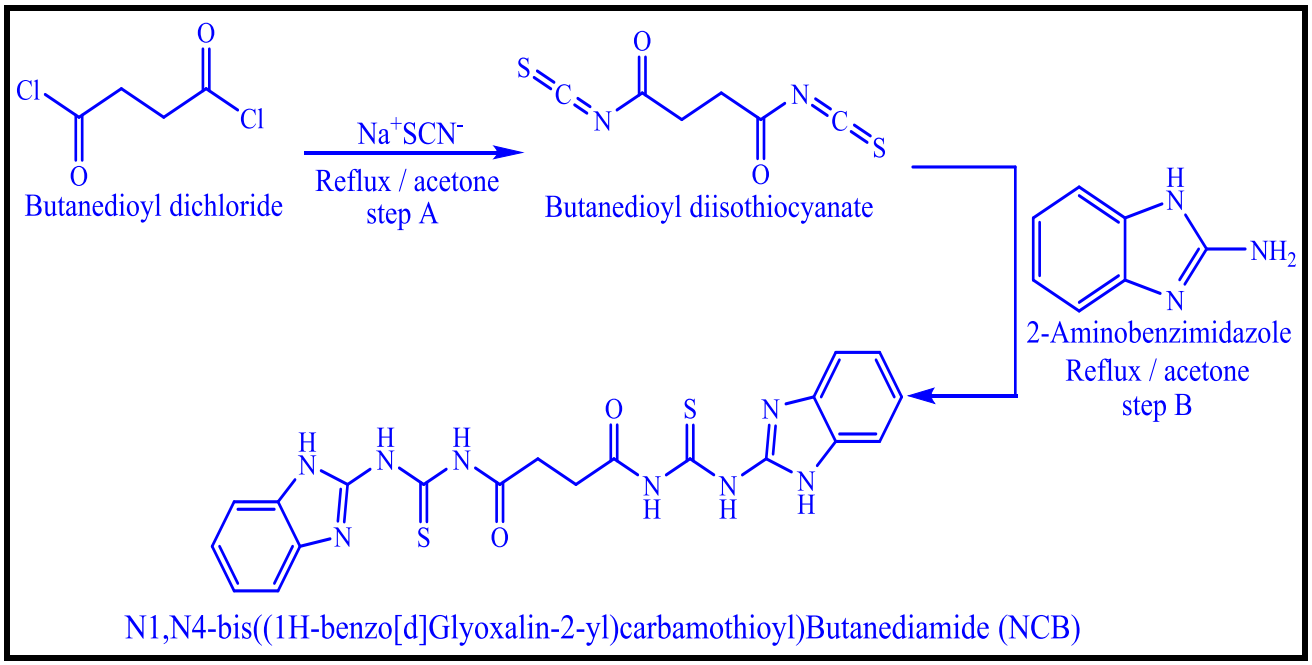


**Scheme 1: Preparation course of the (NCB)**

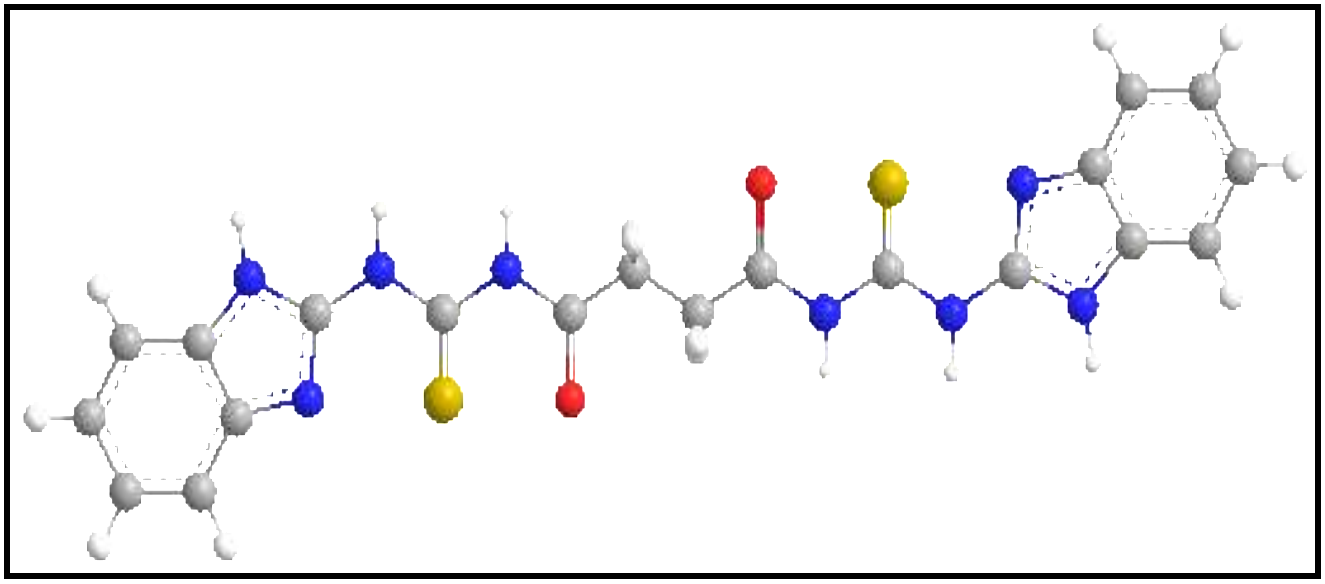

**Fig.1: 3D –Structure of the (NCB)**

## The In-Organic Compounds

### Synthesis of [Ni (NCB)] $Cl_2$

To a (10 ml) ethanolic solution (0.933g, 2mmol) of (NCB), (10 ml) ethanolic solution (0.475g, 2mmol) of Nickel (II) chloride have been added with heating and stirring for 4h.After the products were filtered and then washed and recrystallized by absolute ethanol and finally in a vacuum over the silica gel was dried. For the preparation of complexes of (NCB) with Cr(III), Mn(II) Co(II), Cu(II), Pd(II), Ag(I), Cd(II) ion, a similar procedure in the preparation of Ni (II) was used, but in (1:1) (M:L) mole ratio, Fig.(2,3).

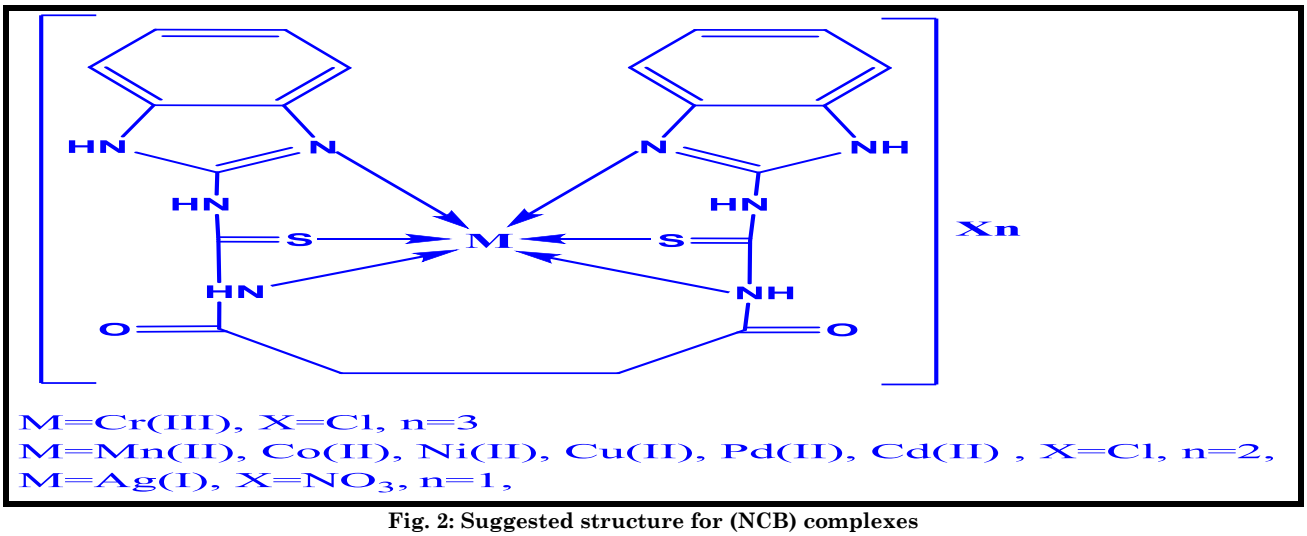


**Fig. 2: Suggested structure for (NCB) complexes**

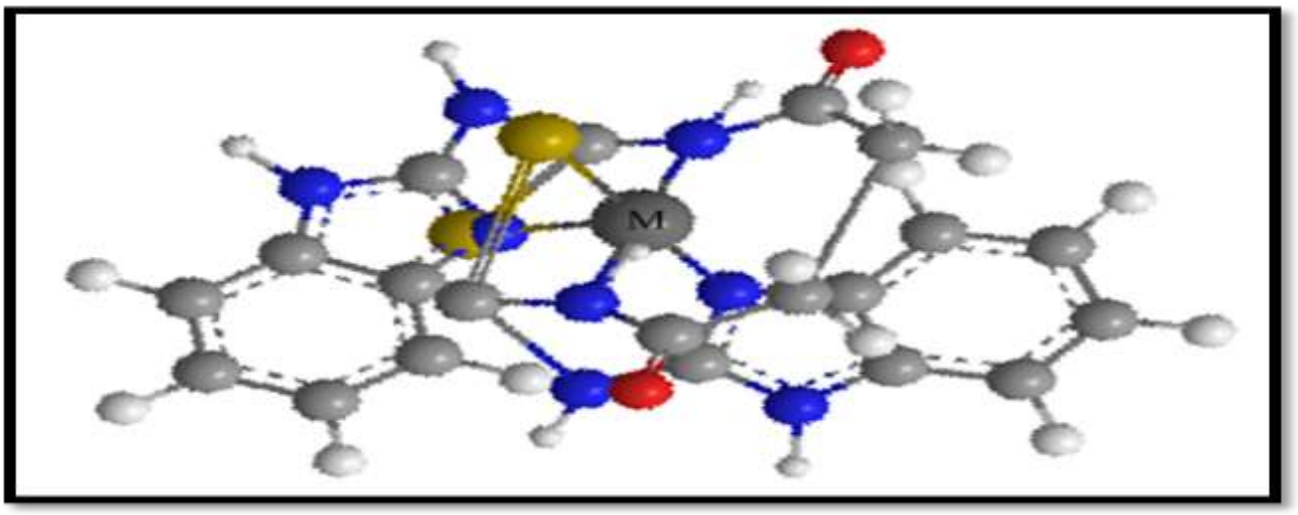


**Fig.3: 3D structure of (NCB) complexes**

**Table 1: Some physical data, percentage of metal (%M), melting point and molar conductivity of the prepared compounds**

| Compound | Empirical Formula (Formula wt.) | m.p(°C) or d | Color | Metal% Calculated (Actual) | Conducts $Ohm^{-1}cm^2mol^{-1}$ in solvent (DMSO) |
|---|---|---|---|---|---|
| Ligand (NCB) | $C_{20}H_{18}N_8O_2S_2$ 466.54 | 225-227 | Yellow | ----- | ----- |
| $[Cr(NCB)]Cl_3$ | $C_{20}H_{18}Cl_3CrN_8O_2S_2$ 624.88 | 265-267 | Green | 8.32 (8.37) | 210 |
| $[Mn(NCB)]Cl_2$ | $C_{20}H_{18}Cl_2MnN_8O_2S_2$ 592.38 | 268-270 | Brown | 9.27 (9.21) | 111.2 |
| $[Co(NCB)]Cl_2$ | $C_{20}H_{18}Cl_2CoN_8O_2S_2$ 596.37 | 276-278 | Green | 9.88 (9.82) | 167.6 |
| $[Ni(NCB)]Cl_2$ | $C_{20}H_{18}Cl_2NiN_8O_2S_2$ 596.13 | 253-255 | Green | 9.85 (9.84) | 143.8 |
| $[Cu(NCB)]Cl_2$ | $C_{20}H_{18}Cl_2CuN_8O_2S_2$ 600.98 | 340 d | Brown | 10.57 (10.51) | 152.9 |
| $[Pd(NCB)]Cl_2$ | $C_{20}H_{18}Cl_2PdN_8O_2S_2$ 643.86 | 335 d | Brown | 16.53 (16.49) | 138.6 |
| $[Ag(NCB)]NO_3$ | $C_{20}H_{18}AgN_9O_5S_2$ 636.41 | 285-287 | Brown | 16.95 (16.92) | 65.3 |
| $[Cd(NCB)]Cl_2$ | $C_{20}H_{18}Cl_2CdN_8O_2S_2$ 649.85 | 310 d | Yellow | 17.30 (17.35) | 141.2 |

d= decomposition

## Results and Discussion

One of the most important characteristics of mineral complexes is that it is thermally stable and solid color. They are soluble in Dimethyl formamide and Dimethyl sulphoxide. The theoretical and practical results of atomic absorption measurements for all prepared complexes were approximated, Table (1).

### NMR Spectra

### $^1$H-NMR Spectra of (NCB)

The integral intensities of each signal in $^1$HNMR spectrum of (NCB) Fig (4).Was found to agree with the number of different types of protons present. The spectrum showed the singlet signal at (δ=8.59 ppm) is assigned to (1H, NH sec. amide). The multiplied signal of the aromatic protons were assigned in range (δ=7.19-7.59 ppm). The chemical shift of amine group, (1H, NH sec. amine) appeared in range (δ=2.43-2.52 ppm).

The signal at chemical shift (δ=6.84 ppm) is determined to the proton of (NH in ring) group. Finally the signal at chemical shift (δ=2.63 ppm) is determined to group protons ($CH_2$) [10-11]. The results are summarized in Table (2).

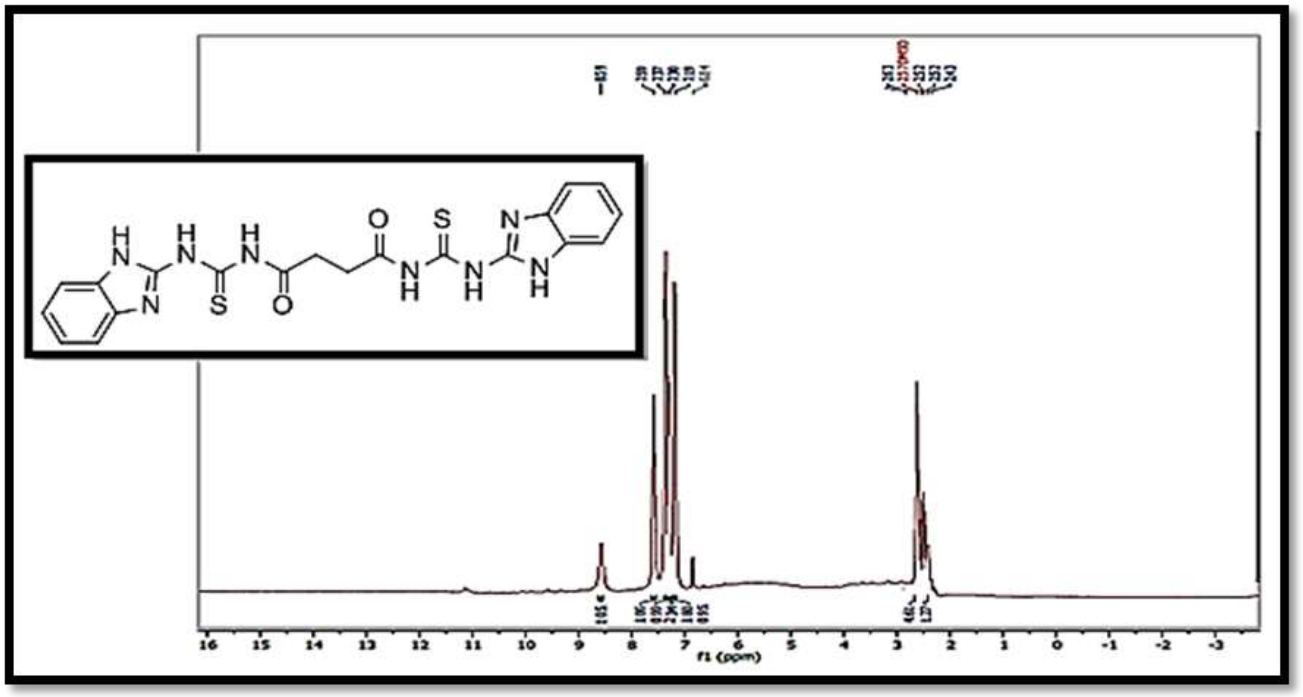


**Fig. 4: $^1$H-NMR spectra of (NCB)**

 

**Table 2: $^{1}$H-NMR data for (NCB) measured in DMSO-d$^{6}$ and chemical shift in ppm (δ)**

| Comp. | Functional groups | δ (ppm) |
|---|---|---|
| (NCB) | 1H, NH sec. amide | 8.59 |
| | aromatic protons | 7.19-7.59 |
| | 1H, NH sec. amine | 2.43-2.52 |
| | 1H, N-H in ring group | 6.84 |
| | 2H ,$CH_2$ group | 2.63 |

## $^{13}$C-NMR Spectra of (NCB)

$^{13}$C-NMR spectrum of (NCB), Fig.(5) in $(CD_3)_2SO$ solvent shows that the chemical shift at (δ= 174.04 ppm) attributed to ($C_1$) for C=S group. The ($C_2$) for C=O group resonated with the chemical shift at (172.48 ppm).

The ($C_3$, $C_4$, $C_5$, $C_6$) resonated with the chemical shift at (δ= 150.84, 144.15, 123.40, 111.75 ppm) respectively. Finally the chemical shift at ((δ= 38.87-39.15 ppm) attributed to ($C_7$) [12, 13], Fig. (3).The results are summarized in Table (3).

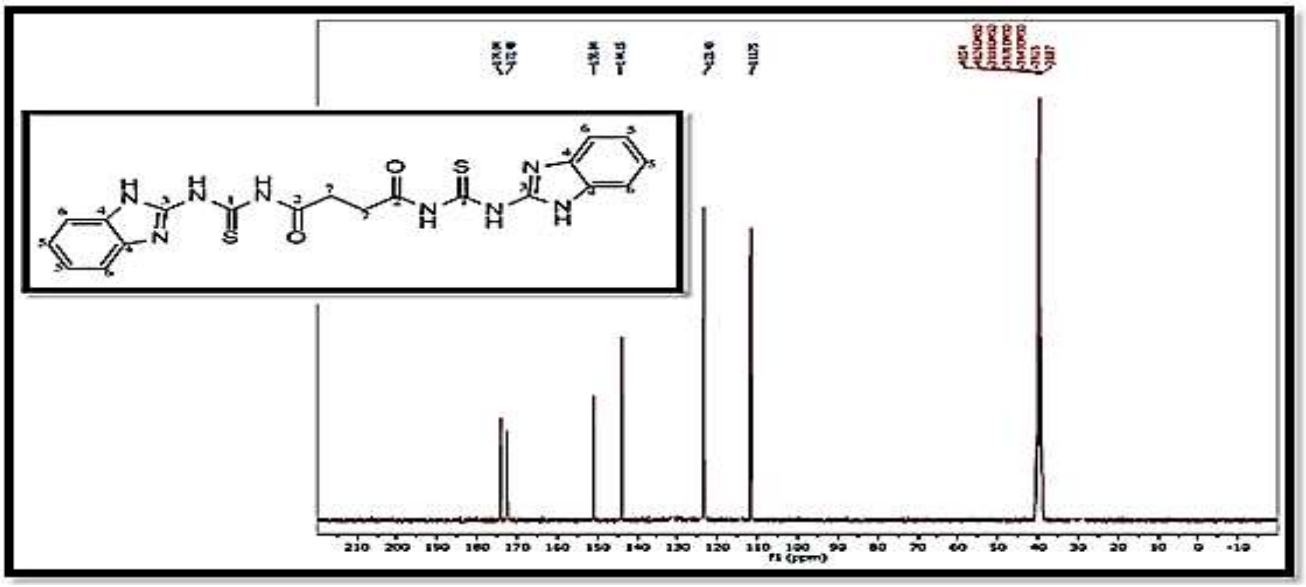

**Fig.5: $^{13}$C-NMR spectra of (NCB)**

**Table 3: $^{13}$C-NMR data for (NCB) measured in DMSO-d$^{6}$ and chemical shift in ppm (δ)**

| Comp. | Functional groups | δ (ppm) |
|---|---|---|
| (NCB) | $C_1$ for C=S group | 174.04 |
| | $C_2$ for C=O group | 172.48 |
| | $C_3$ for N-C=N group | 150.84 |
| | $C_4$ for (Ar- ring) | 144.15 |
| | $C_5$ for (Ar- ring) | 123.40 |
| | $C_6$ for (Ar- ring) | 111.75 |
| | $C_7$ for $CH_2$ group | 38.87-39.15 |

## FT-IR Spectra

## Ligand (NCB)

The band at (3390) cm$^{-1}$ in the spectrum of the (NCB) determined to the υ(NH), while another absorption band showed at (1681) cm$^{-1}$ could be interpreted as υ(C=O) , in addition to absorption bands at (1604) and (1037) cm$^{-1}$ which determined to υ(C=N in ring),(C=S) respectively [14,15 ], Fig.(6).

## Complexes of ligand (NCB)

These spectra showed a marked various between bands belonging to the stretching vibration of υ(NH, amide group) in the range between (3472-3417) cm$^{-1}$ shifted to higher frequencies by (82-27) cm$^{-1}$ proposing the probability of the co-ordination of (NCB) by the nitrogen atom at the amide group [16,17] ,The stretching vibration band υ(C=N) has been found in the range (1635-1627) cm$^{-1}$ shifted to higher frequencies by (31-23) which means the nitrogen atom of (C=N in ring) was involved in the coordination [18].

The stretching vibration band υ(C=S) was found in the range (1091-1061) cm$^{-1}$ shifted to a higher frequency by (54-24) cm$^{-1}$ which means that the sulfur atom was involved in the coordination [19, 20]. The υ C=O in ligand was not correlated with the central ion and was confirmed by no changes in the frequencies of this group that were set at (1685-1678) cm$^{-1}$ in the complexes. In the

 

spectrum of the ligand complexes, new bands υ(M-S) ,υ(M-N ,in ring) and υ(M-N ,amide group) appeared in the range of (449-437) $cm^{-1}$, (536-505) $cm^{-1}$ and (609-543) $cm^{-1}$ respectively [21,22]. Co-ordination through the sulfur atom in the group (C=S), the nitrogen atom in the group (NH-C=O), the nitrogen atom in the group (C=N in the ring) with the metal ions resulted in the emergence of new bands indicating the formation of the metal complexes [23]. In Table (4), FT-IR data is displayed. In Fig.(6, 7), the spectra of the (NCB) and its complexes were presented.

**Table 4: FT-IR data of (NCB) ($cm^{-1}$) and their complexes**

| Comp. | υ N–H (amide) | υ C=O | υ C=N (in ring) | υ C=S | υ M-S | υ M-N |
|---|---|---|---|---|---|---|
| Ligand (NCB) | $3390_{(s)}$ | $1681_{(s)}$ | $1604_{(m)}$ | $1037_{(m)}$ | ------ | ------ |
| $[Cr(NCB)]Cl_3$ | $3417_{(b)}$ | $1681_{(s)}$ | $1628_{(m)}$ | $1091_{(m)}$ | $439_{(m)}$ | $513_{(w)}$ $553_{(m)}$ |
| $[Mn(NCB)]Cl_2$ | $3417_{(b)}$ | $1678_{(s)}$ | $1629_{(s)}$ | $1068_{(w)}$ | $443_{(w)}$ | $536_{(w)}$ $559_{(m)}$ |
| $[Co(NCB)]Cl_2$ | $3453_{(s)}$ | $1681_{(s)}$ | $1631_{(m)}$ | $1072_{(m)}$ | $443_{(m)}$ | $524_{(m)}$ $578_{(w)}$ |
| $[Ni(NCB)]Cl_2$ | $3464_{(b)}$ | $1681_{(s)}$ | $1632_{(m)}$ | $1068_{(w)}$ | $439_{(w)}$ | $524_{(w)}$ $547_{(m)}$ |
| $[Cu(NCB)]Cl_2$ | $3471_{(s)}$ | $1679_{(s)}$ | $1631_{(s)}$ | $1061_{(m)}$ | $437_{(w)}$ | $522_{(m)}$ $609_{(w)}$ |
| $[Pd(NCB)]Cl_2$ | $3429_{(b)}$ | $1679_{(s)}$ | $1627_{(m)}$ | $1072_{(m)}$ | $449_{(m)}$ | $513_{(m)}$ $543_{(w)}$ |
| $[Ag(NCB)]NO_3$ | $3433_{(s)}$ | $1685_{(s)}$ | $1635_{(s)}$ | $1072_{(w)}$ | $447_{(w)}$ | $505_{(m)}$ $559_{(w)}$ |
| $[Cd(NCB)]Cl_2$ | $3472_{(b)}$ | $1678_{(s)}$ | $1627_{(m)}$ | $1068_{(w)}$ | $443_{(m)}$ | $536_{(m)}$ $555_{(w)}$ |

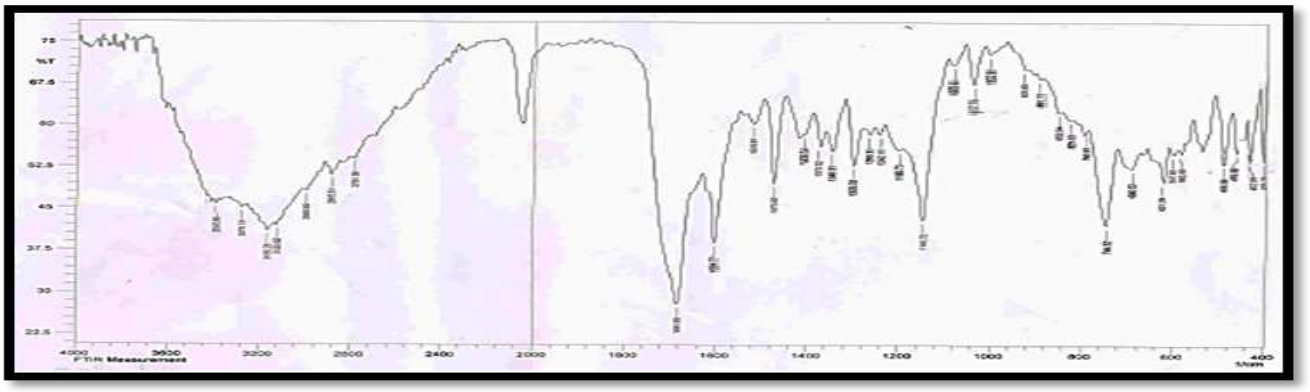

**Fig. 6: Fourier-transform infrared spectrum of (NCB)**

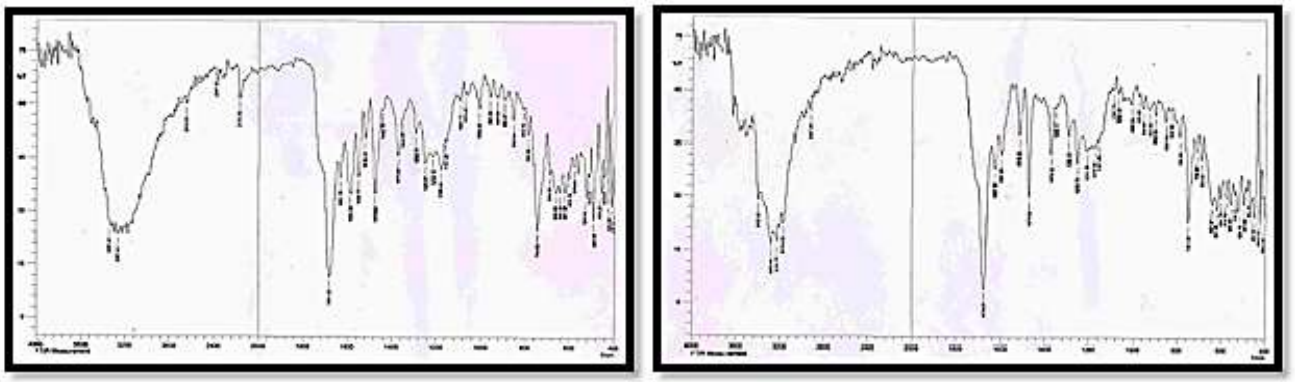

**Fig.7: Fourier-transform infrared spectrum of [Co (NCB)] $Cl_2$, [Cd (NCB)] $Cl_2$ complexes**

## Electronic Spectra

## Ligand (NCB)

The highest absorption intense was found at (35587) and (27932) $cm^{-1}$, Fig.(8) which is due to transitions (π→π*) and (n→π*) respectively, in the electronic spectrum of the (NCB) [24].

In Table (5), data are recorded.

## Complexes of ligand (NCB)

The electronic spectrum of the chromium complex showed bands at (32894, 17241 and 13422) $cm^{-1}$ due to $^4A_2g \rightarrow {}^4T_1g$ (P), $^4A_2g \rightarrow {}^4T_1g$ (f) and $^4A_2g \rightarrow {}^4T_2g$ (f) transitions respectively,

suggesting that it had octahedral geometry [25].

The electronic spectrum of the manganese complex showed bands at (36101, 13422 and 10341) $cm^{-1}$ due to L.F, $^6A_1g \rightarrow {}^4T_2g$ (G) and $^6A_1g \rightarrow {}^4T_1g$ (G) transitions respectively, suggesting that it had octahedral geometry [26]. On the basis of the bands in the cobalt complex at (35971, 28653, 16129 and 11148) $cm^{-1}$, which is back to L.F, C.T mixed with $^4T_1g \rightarrow {}^4T_1g$ (f), $^4T_1g \rightarrow {}^4A_2g$ (f) and $^4T_1g \rightarrow {}^4T_2g$ (f) transitions respectively, the octahedral geometry of the complex was proposed [27].

Regarding the Nickel complex, the electron spectra appear absorption bands may be assigned to L.F, C.T mixed with $^3A_2g \rightarrow {}^3T_1g$ (f) , $^3A_2g \rightarrow {}^3T_1g$ (f) and $^3A_2g \rightarrow {}^3T_2g$ (f) transition which exhibit in (35842, 28653, 23474 and 12674) $cm^{-1}$ respectively. A characterization of these bands indicates that the complex has octahedral geometry [28]. Confirming the octahedral geometry of the copper complex is the appearance of the bands at (33333 and 10905) $cm^{-1}$ are returns to C.T and $^2Eg \rightarrow {}^2T_2g$ transitions [29]. The electronic spectrum of palladium complex appeared bands at (32154, 13106 and 11976) $cm^{-1}$, the former bands are probably due to C.T, $^1A_1g \rightarrow {}^1B_1g$ and $^1A_1g \rightarrow {}^1A_2g$ which indicates the octahedral geometry of this complex [30].

On the basis of bands shown in the electronic spectrum of the silver complex at (36363 and 28089) $cm^{-1}$, which is probably due to C.T, the octahedral geometry of the complex was suggested [31]. The octahedral geometry of the cadmium complex was proposed on the basis of the band that appeared at (35842) $cm^{-1}$ which is back to C.T [32]. In Table (5), UV data was displayed. In Figure (8, 9) the spectra of the (NCB) and its complexes were displayed.

**Table 5: UV-Vis data of (NCB) and their complexes**

| Comp. | λ(nm) | υ(cm$^{-1}$) | $\varepsilon_{max}$ (molar$^{-1}$ .cm$^{-1}$) | Transitions | ($\mu$eff B.M) |
|---|---|---|---|---|---|
| Ligand (NCB) | 281 | 35587 | 1942 | $\pi \rightarrow \pi^*$ | ------- |
| | 358 | 27932 | 371 | $n \rightarrow \pi^*$ | |
| $[Cr(NCB)]Cl_3$ | 304 | 32894 | 1939 | $^4A_2g \longrightarrow {}^4T_1g_{(P)}$ | 3.70 |
| | 580 | 17241 | 29 | $^4A_2g \longrightarrow {}^4T_1g_{(f)}$ | |
| | 745 | 13422 | 4 | $^4A_2g \longrightarrow {}^4T_2g_{(f)}$ | |
| $[Mn(NCB)]Cl_2$ | 277 | 36101 | 1718 | L.F | 5.96 |
| | 745 | 13422 | 23 | $^6A_1g \longrightarrow {}^4T_2g_{(G)}$ | |
| | 967 | 10341 | 3 | $^6A_1g \longrightarrow {}^4T_1g_{(G)}$ | |
| $[Co(NCB)]Cl_2$ | 278 | 35971 | 2331 | L.F | 4.85 |
| | 349 | 28653 | 1328 | $C.T_{mixed\ with}{}^4T_1g_{(F)} \longrightarrow {}^4T_1g_{(P)}$ | |
| | 620 | 16129 | 75 | $^4T_1g_{(F)} \longrightarrow {}^4A_2g$ | |
| | 897 | 11148 | 4 | $^4T_1g_{(F)} \longrightarrow {}^4T_2g_{(F)}$ | |
| $[Ni(NCB)]Cl_2$ | 279 | 35842 | 1813 | L.F | 2.97 |
| | 349 | 28653 | 119 | $C.T_{mixed\ with}{}^3A_2g \longrightarrow {}^3T_1g_{(P)}$ | |
| | 426 | 23474 | 68 | $^3A_2g \longrightarrow {}^3T_1g_{(F)}$ | |
| | 789 | 12674 | 7 | $^3A_2g \longrightarrow {}^3T_2g_{(F)}$ | |
| $[Cu(NCB)]Cl_2$ | 300 | 33333 | 2242 | C.T | 1.82 |
| | 917 | 10905 | 77 | $^2Eg \longrightarrow {}^2T_2g$ | |
| $[Pd(NCB)]Cl_2$ | 311 | 32154 | 2434 | C.T | 0 |
| | 763 | 13106 | 11 | $^1A_1g \longrightarrow {}^1B_1g$ | |
| | 835 | 11976 | 8 | $^1A_1g \longrightarrow {}^1A_2g$ | |
| $[Ag(NCB)]NO_3$ | 275 | 36363 | 1089 | C.T | 0 |
| | 356 | 28089 | 342 | C.T | |
| $[Cd(NCB)]Cl_2$ | 279 | 35842 | 1839 | C.T | 0 |

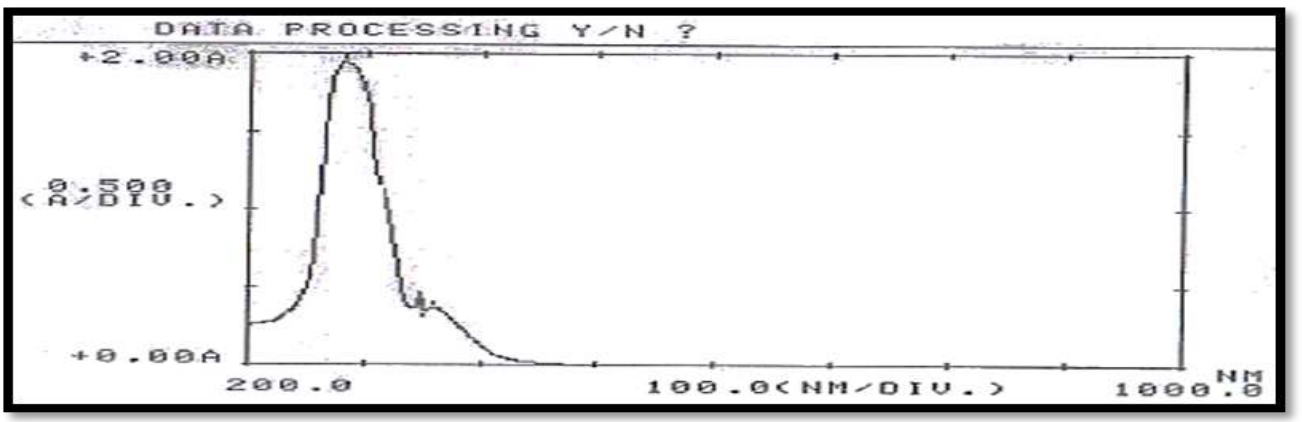


**Fig. 8: Electronic spectrum of (NCB)**

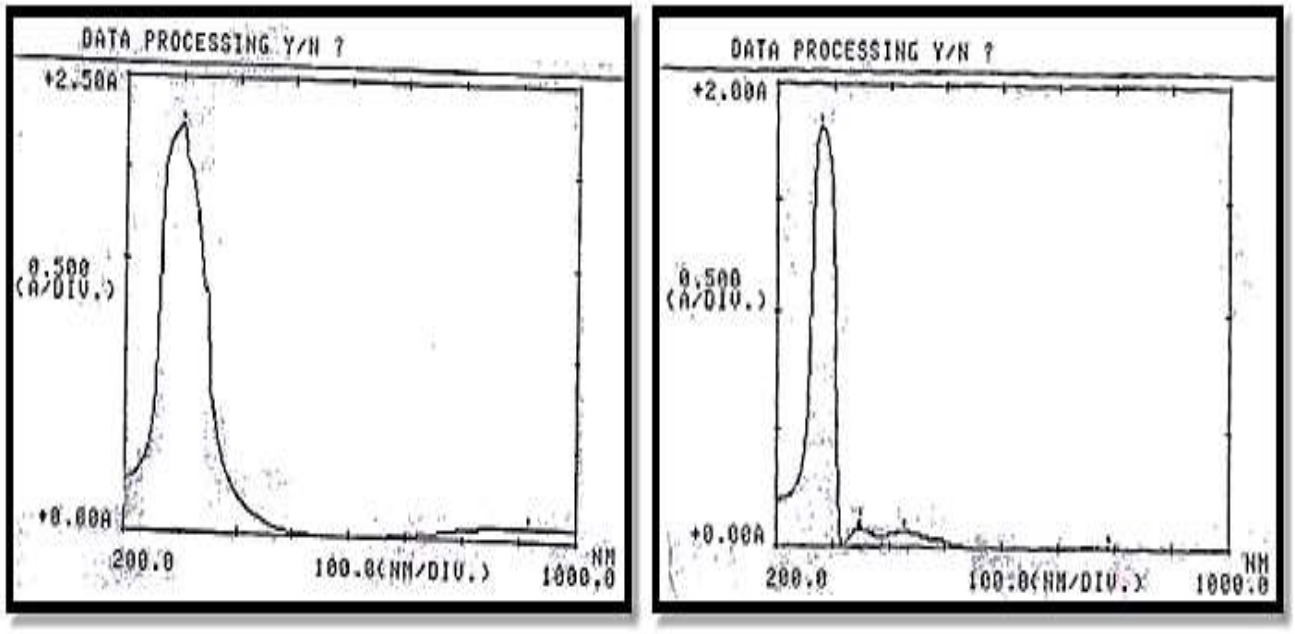


**Fig. 9: Electronic spectrum of [Cu (NCB)] $Cl_2$, [Ni (NCB)] $Cl_2$ complexes**

## Magnetic Moments and Conductivity Measurements

In Table (5), the values of measured magnetic susceptibility and the effective magnetic moment (μeff) for Cr (III), Mn (II), Co (II), Ni (II), and Cu (II) complexes are displayed. These complexes exhibit μeff (3.70, 5.96, 4.85, 2.97 and 1.82) B.M respectively, these normal values are consistent with high spin octahedral complexes [33]. The electrolytes nature ((1:3) ;$Cr^{+3}$ complex, (1:2); $M^{+2}$= Mn(II), Co(II), Ni(II), Cu(II), Pd(II) and Cd(II) complexes,(1:1); $Ag^{+1}$ complex) of all metal complexes was confirmed by molecular conductivity measurements [34], Table (1).

## The Role of Ligand (NCB) in Inhibition of Corrosion on Mild Steel in Base Medium

The corrosion of mild steel was studied when immersion in Ca $(OH)_2$ solution saturated with the presence of (NCB) as inhibitor. In a series of solutions $10^{-4}$, $10^{-3}$, $10^{-2}$ M respectively, the inhibitor efficiency of the (NCB) was tested. Within these ranges of concentrations, The (NCB) showed greater inhibiting properties for corrosion. By reducing the working concentration below the range of $10^{-4}$ M, minimum inhibitor concentration was found. The results of percentage inhibition efficiency (%I.E) indicate that the (NCB) is good inhibitor. The inhibition mechanism is ascribed to the adsorption of ($N^+$) on the negative active sites on the metal surface, while the (π–electrons) of the conjugated system adsorbed on the positive active sites of the metal surface [35-37].The inhibition rate follows the order :-

**$Ca(OH)_2$ + L($10^{-2}$M) > $Ca(OH)_2$ + L($10^{-3}$M) > $Ca(OH)_2$ + L($10^{-4}$M) > $Ca(OH)_2$ saturated**

Where L =Ligand (NCB)

The results of the immersion process for 48 h resulting from the weight loss were included in Table (6).

**Table 6: Data of Weight before and after immersion of (NCB) on mild steel in $Ca(OH)_2$ solution at laboratory temperature.**

| Solutions | Weight before immersion | Weight after immersion | Weight difference | Percentage of weight loss | Percentage of E.I |
|---|---|---|---|---|---|
| $Ca(OH)_2$+L($10^{-2}$M) | 0.7567 | 0.6023 | 0.1544 | 20.40 | 20.90 |
| $Ca(OH)_2$+L($10^{-3}$M) | 0.7713 | 0.6054 | 0.1659 | 21.51 | 15.01 |
| $Ca(OH)_2$+L($10^{-4}$M) | 0.7617 | 0.5801 | 0.1816 | 23.38 | 6.96 |
| $Ca(OH)_2$ control | 0.7658 | 0.5706 | 0.1952 | 25.48 | - |

## Thermal Analysis

The ligand (NCB) was prepared and some of its selected complexes were subjected to thermal analysis using a STAPT-1000 Linseis company1 Germany. In an atmosphere of argon gas, this measurement was done within temperature range (0-600)°C and heating rate 10°C/min [38,39]. Where it was recorded all results are derived from the TG curves for these compounds examined in Table (7), Fig (10-12).

**Table 7: Temperature values for analysis along with corresponding weight loss values.**

| Compounds | Stage | TGA | | | |
|---|---|---|---|---|---|
| | | TG range(°C) | Found (calculate) | | Assignment |
| | | | Mass loss | % Mass loss | |
| Ligand (NCB) | 1 | 30-595 | 8.849 (8.845)<br>9.492 (9.487) | 52.056<br>(52.029) | - $C_7H_{15}N_8O_2$ |
| [Cr(NCB)]$Cl_3$ | 1 | 80-330 | 3.026 (3.025)<br>2.689 (2.675) | 95.051<br>(94.920) | - $C_{10}H_9Cl_3N_8S$ |
| | 2 | 331-451 | 10.621<br>(10.594) | | - $C_7H_5S$ |
| | 3 | 452-596 | 3.370<br>(3.355) | | - $C_4H_7Cr$ |
| [Co(NCB)]$Cl_2$ | 1 | 110-420 | | 73.638<br>(73.422) | - $C_{10}H_6Cl_2N_8S$ |
| | 2 | 421-596 | | | - $C_6H_4S$ |

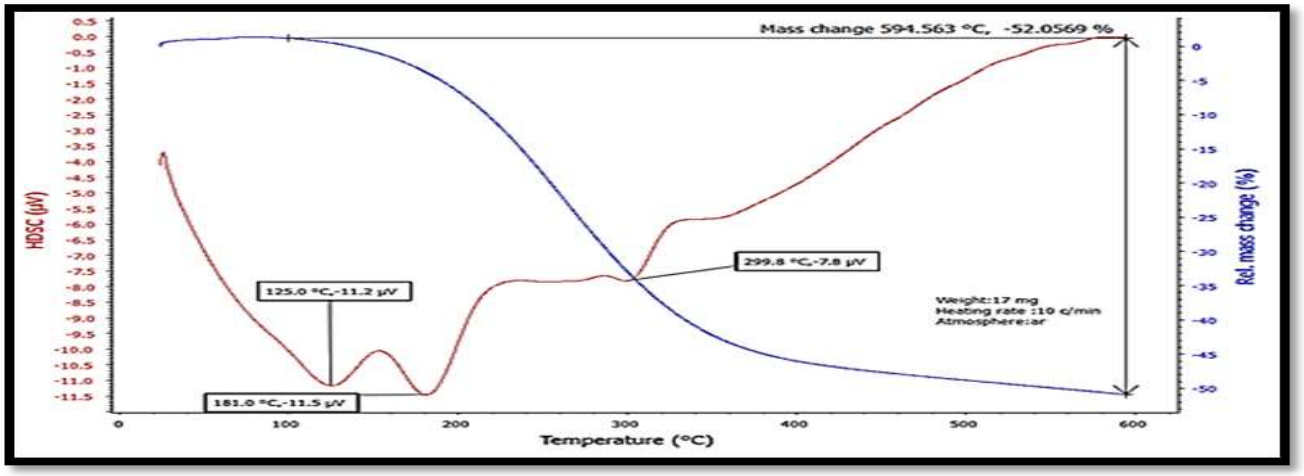


**Fig. 10: Thermal study of (CNB)**

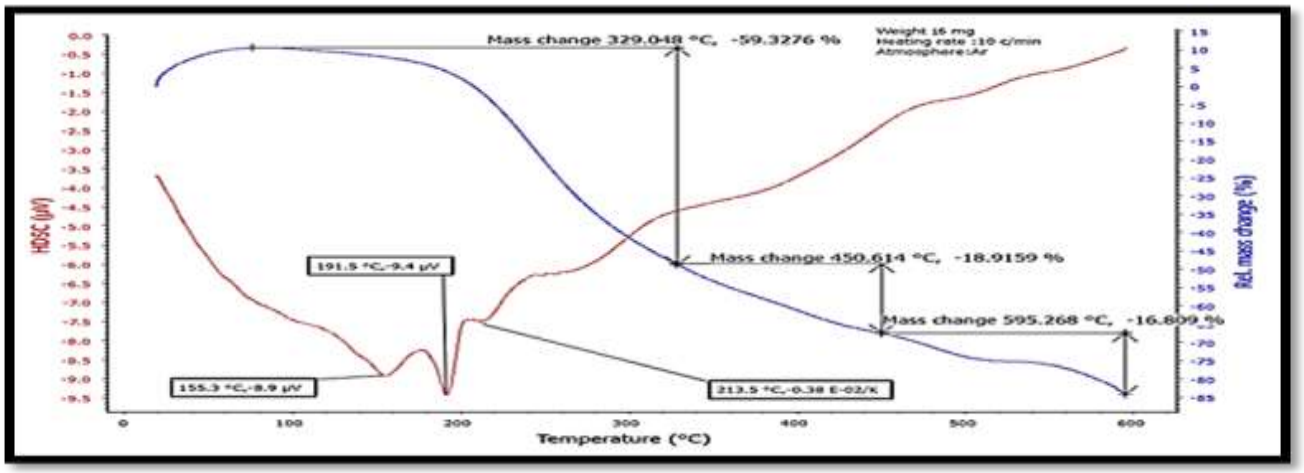


**Fig.11: Thermal study of [Cr (NCB)] $Cl_3$ complex**

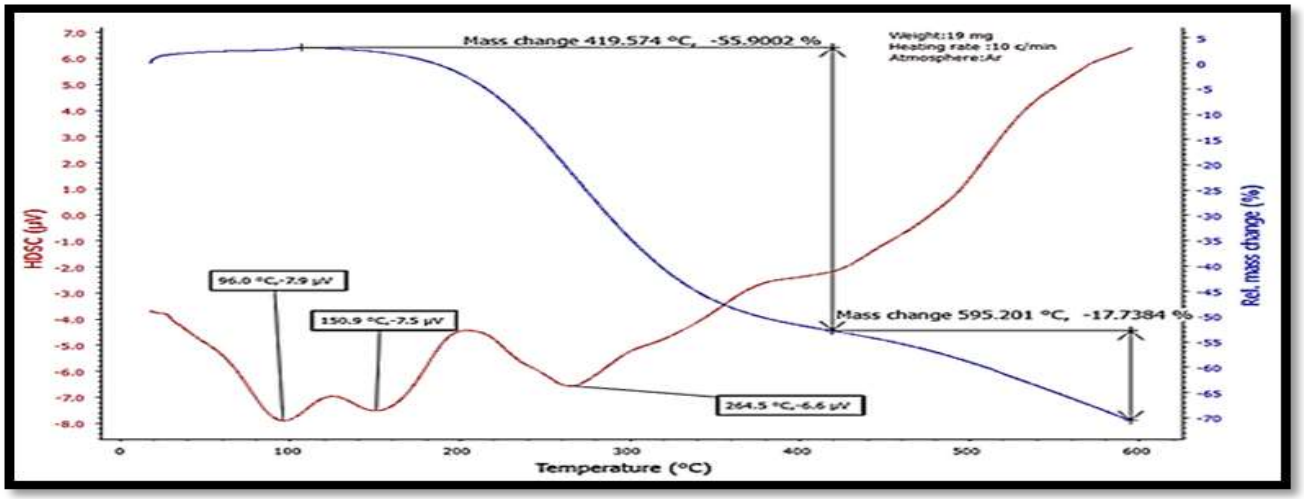


**Fig. 12: Thermal study of [Co (NCB)] Cl2 complex**

## Anti-bacterial Activity Studies

Bacterial cultures and growth conditions, *Escherichia coli* ($G^-$) and *Staphylococcus aureus* ($G^+$) were used as test micro-organisms. In the tested organisms, the medium surface was inoculated and covered. Before applying disks, allow the agar surface to dry from 3 to 5 minutes. Using sterile forceps, the disks were dipped into a beaker of the chemicals and placed them in the previous medium. At 37 °C for 48 hours, Cultures plates of bacteria were incubated to grow. In concentrations prepared, the complexes display high efficacy to inhibit the spread of bacteria compares ligand (NCB) [40-42]. The data obtained are found in the Table (8), Fig (13, 14).

**Table 8: The diameter values of inhibition of the (NCB) and some complexes prepared**

| No. | Compounds | *Escherichia coli* | *Staphylococcus aureus* |
|---|---|---|---|
| | Control | zero | zero |
| 1 | Ligand (NCB) | 15(D) | 12(D) |
| 2 | $[Cr(NCB)]Cl_3$ | 15 | 20 |
| 3 | $[Ni(NCB)]Cl_2$ | 24 | 14 |
| 4 | $[Ag(NCB)]NO_3$ | 14 | 20 |

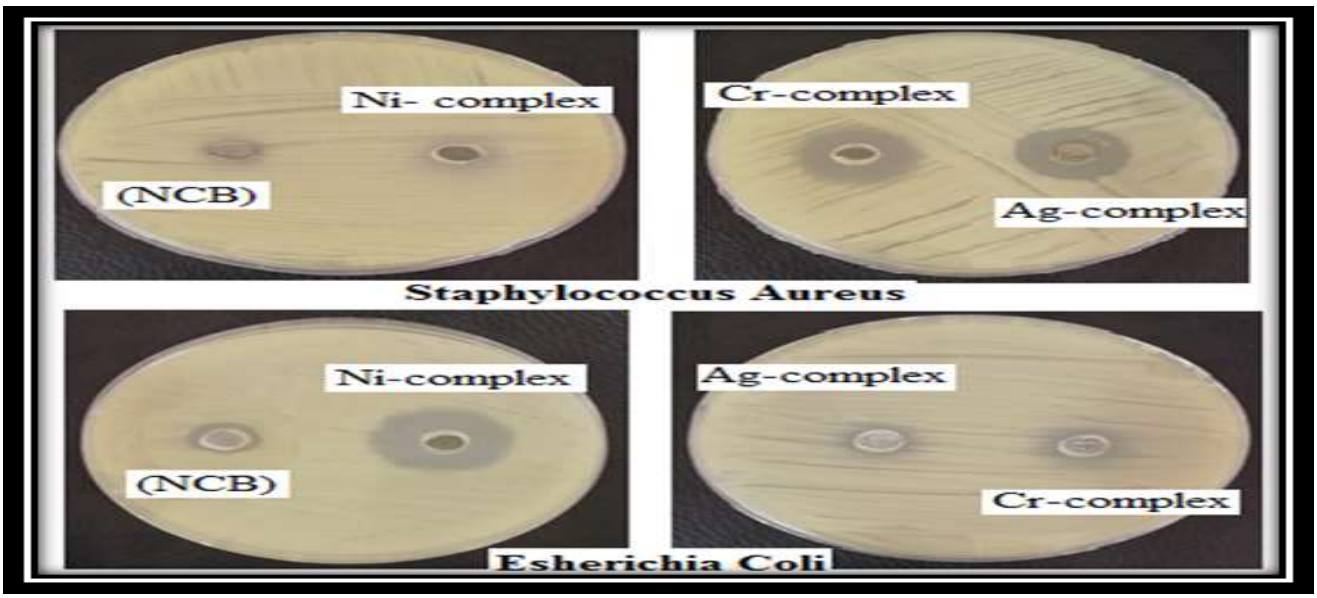


**Fig.13: The diameter values of inhibition of the (NCB) and some complexes prepared against selected bacteria**

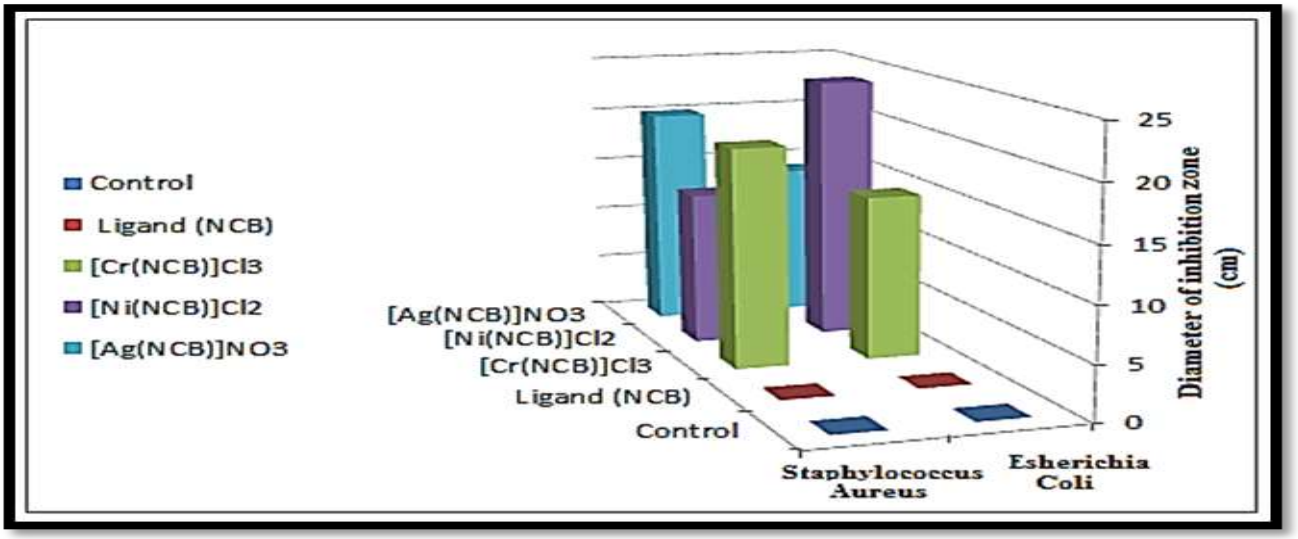


**Fig.14: Statistical representation for biological activity of (CNB) and some metal complexes**

## Conclusion

This paper describes the prepared and identification of a new (NCB) and its Cr(iii), Mn(ii), Co(ii), Ni(ii), Cu(ii), Pd(ii), Ag(i), Cd(ii) complexes. The octahedral geometry of the prepared complexes was suggested on the basis of data ($^1H$-$^{13}C$ NMR for (NCB) only), conductance and magnetic moment for the compounds. The (NCB) acts as hexadentate and coordinates by the S atom in the (C=S) group, N atom in (NH-C=O) group, N atom in (C=N in ring) group. The (NCB) show

 

appreciable corrosion inhibition action against corrosion of mild steel in Ca $(OH)_2$ solution. Multi-step decomposition patterns for their organic frameworks, TGA studies show for (NCB) and its complexes. The (NCB) and its complexes were examined for their anti-bacterial activities against two types of bacteria. The results of these studies showed that their complexes are more activity than free ligand.

## Acknowledgement

The authors express their sincere thanks and appreciation to the College, its distinguished professors and to the laboratory workers for their assistance and support to carry out all research measurements.

## References

1. Kokila RB, Princess R, Suman A (2019) Synthesis, characterization and biochemical studies of metal complexes derived from 2-amino benzoimidazole derivative, Res. J. Chem. Environ., 23 (3):26-35.
2. Garima S, Manjul S (2018) Microwave Assisted Synthesis and Character -ization of Schiff Base of 2-Amino Benzimidazole, Int. J. Pharm. Sci. Drug Res, 10(4): 293-296.
3. Durosinmi LM, Oluduro AO, Oseni M (2017) Synthesis, Characterization and Antimicrobial Properties of Benzimidazole Derivatives and Their Metal Complexes, IOSR Journal of Applied Chemistry, 10(8): 24-45.
4. Muayed AR, Maha S, Ashraf T (2018) Synthesis, spectroscopic characterization, and antibacterial evaluation of new Schiff bases bearing benzi midazole moiety, Journal of Physics: Conf. Series, 10(3): 29-34.
5. Khalid J (2015) Preparation and Characterization of Some Transition Metal Complexes with NovelAzo-Schiff base Ligand Derived from 2(E)-(1H-benzo[d] imidazole-2-yly diazenyl)-5-((E)-benzylideneimino)phenol, RJPBCS,6(5):1298-1308.
6. Alejandro C, Itzia I, Gerardo G (2014) Synthesis and Structure of Sulfur Derivatives from 2-Aminobenzimidazole, Molecules, 19: 13878-13893.
7. Klodian X, Matjaz F (2017) The first electrochemical and surface analysis of 2-aminobenzimidazole as a corrosion inhibitor for copper in chloride solution, New J. Chem., 41: 7151-7161.
8. Musa EM, Kamal KT (2015) Computational Simulation of the Molecular Structure of Benzimidazole and Substituted Benzimidazoles as Corrosion Inhibitors for Brass in Perchloric Acid, American Journal of Research Communication, 3(4):143-152.
9. Imran F, Bohari MY, Siti AH (2017) A comparative study of the metal binding behavior of alanine based bis-thiourea isomers, Chemistry Central Journal, 11(76): 1-16.
10. Ragab RA, Ahmed AM, Yamany BY (2016) Spectral, Thermal and Antibacterial Studies for Bivalent Metal Complexes of Oxalyl, Malonyl and Succinyl-bis-4-phenylthiosemicarbazide Ligands, Open Journal of Inorganic Chemistry, 6: 89-113.
11. Walaa HM, Reem GD, Gehad GM (2016) Novel Schiff base ligand and its metal complexes with some transition elements. Synthesis, spectroscopic, thermal analysis, antimicrobial and in vitro anticancer activity, Appl. Organometal. Chem., 30, 221-230.
12. Suman M, Archana S, Nayaz A (2015) Spectral characterization and thermal behavior of Schiff base metal complex derived from 2-aminobenzimidazole, Advances in Applied Science Research, 6(8):199-204.
13. Naderi R, Mahdavian M, Attar M.M (2009) Electrochemical behavior of organic and inorganic complexes of Zn (II) as corrosion inhibitors for mild steel: Solution phase study, Electrochimica Acta, 54: 6892-6895.
14. Satyendra NS, Pratiksha G, Mahender P (2007) Synthesis and spectroscopic studies of some halogen-dimethylsulphoxide/tetramethylenesulphoxideruthenium (II) and ruthenium (III) complexes with 2-aminobenzimidazoley, Journal of Coordination Chemistry, 60(10): 1047-1055.
15. Shraddha RG, Punita M, Vinod PS (2017) Structural, theoretical and corrosion inhibition studies on some transitionmetal

 

complexes derived from heterocyclic system, Journal of Molecular Structure,7(10): 45-57.

16. Moslem HM, Haitham KD (2014) Synthesis and spectral characterization of some metal complexes containing azo derived from 2-amino benzimidazole, AL-Qadisiyha Journal For Science ,19 (2): 86-96.
17. Nakamato K (1997) Infrared Spectra of Inorganic and Coordination Compounds. Fifth Edition. John Wiley and Sons, New York.
18. Noor, S. H. and Sheikh, A. I. , (2018) Synthesis, Structural, Density Functional Theory, and X-Ray Diffraction Study of Zn(II) N-Isopropylbenzyldithiocarbamate: Anti-Corrosion Screening in Acid Media, Indones. J. Chem., 18 (4): 755-765.
19. Fawaz AS (2014) Co-ordination Chemistry of Some First Row Transition Metal Complexes with Multi-dentate Ligand (1-benzoyl - 3-(4-methylpyridin -2-yl) thiourea), Spectral, Electrochemical and X-ray Single Crystal Studies, Int. J. Electrochem. Sci., 9: 4761-4775.
20. Alia SK, Ibtisam JD, Manhel RA (2013) Synthesis and Characterization of some Mixed Ligand Complexes Containing (8-hydroxyquinoline) and (2-picoline) with some Metal Ions, Baghdad Science Journal, 10(2):396-404.
21. Caspar N, Deacon AD (2017) Synthesis and Structures of Rare Earth 3-(49-Methylbenzoyl)-propanoate Complexes– New Corrosion Inhibitors, Aust. J. Chem., 70: 478-484.
22. Taghreed MM (2016) Synthesis, Characterization and Thermal Study of Some Transition Metal Complexes Derived from Quinoxaline-2, 3-Dione, Ibn Al-Haitham Journal for Pure and Applied science, 8(4):206-220.
23. Silverstein RM, Bassler GC, Morrill TG (1980) Spectrometric Identification of Organic Compound. Fourth Edition. John-Wiley and Sons, Inc., New York, London.
24. JOSE CV, JOY TA (2009) Studies on Complexes of CuII and ZnII metal ions with 2-(thiophene-2-formylimino) benzimidazole, Int. J. Chem. Sci., 7(4): 2541-2548.
25. Hanan FA, Nour FA (2012) Synthesis, spectroscopic, thermal characterization and antimicrobial activity of miconazole drug and its metal complexes, J. Therm. Anal. Calorim, 109: 883-892.
26. Pooja S, Ashish K (2013) Synthesis, structural and corrosion inhibition properties of some transition metal(II) complexes with o-hydroxyacetophenone-2-thiophenoyl hydrazine, Polyhedron, 65 :73-81.
27. Raziyeh AA, Saeid A (2012) Synthesis, Spectroscopy, Thermal Analysis, Magnetic Properties and Biological Activity Studies of Cu (II) and Co (II) Complexes with Schiff Base Dye Ligands, Molecules, 17: 6434-6448.
28. Wan G, Bin X, Chong X (2019) Thermal Stability of $[Ni(htde)](ClO_4)_2$ and Its Corrosion Inhibition Effect for Mild Steel in 1.0 M HCl and $H_2SO_4$ Solutions, Int. J. Electrochem. Sci., 14: 494-505.
29. Wasan MA (2018) Synthesis, Characterization and the Corrosion Inhibition Study of Two Schiff Base Ligands Derived From Urea and Thiourea and Their Complexes with Cu(II) and Hg(II) Ions, Journal of Physics: Conference Series, 7(3):1-16.
30. Jelena MM, Pavle ZM, Tatyana VK (2018) Thermal Analysis, Antioxidant and in vitro Antimicrobial Activity of Palladium (II) Complexes with N, N'- Ethylenediamine Bidentate Ester Ligands, Der Chemica Sinica, 9(1):535-543.
31. Ume F, Moumita P, Ji YR (2017) Synthesis and Photophysical Study of an Octahedral Silver(I) 1-D Coordination Polymer with Thiocarboxylic-Acid-Based Ligands, Polyhedron, 5(2): 57-79.
32. Mriganka D, Amrita B, Bidyut K (2017) Synthesis of cadmium (II) Schiff base complexes towards corrosion inhibition on mild steel, RSC Adv., 7: 48569-48585.
33. Nassar AM, Hassan AM, Shoeib MA (2015) Synthesis, Characterization and Anticorrosion Studies of New Homobimetallic Co (II), Ni (II), Cu (II), and Zn (II) Schiff Base Complexes, J. Bio. Tribo. Corros., 1(19):1-16.
34. Yogesh KS, Magan P (2012) Synthesis, Spectral, Cyclic Voltammetric and Antimicrobial Studies of Iron (III) Complexes with Tetradentate Bis-benzimidazole Based Diamide Ligand, Orient. J. Chem., 28(3), 1419-1424.

 

35. Nadra B, Ali O (2017) Crystal Structure and Corrosion Inhibition Properties of Ferrocenyl- and Phenylendiamine-Iminomethylphenoxy Cobalt Complexes, J. Chem. Crystallogr., 47:40-46.

36. Shubham K, Sanjiv K, Kalavathy R (2018) Synthesis, biological evaluation and corrosion inhibition studies of transition metal complexes of Schiff base, Chemistry Central Journal, 12: 117: 1-10.

37. Karimah K, Nurul A, Norsakina ZZ (2017) Synthesis of Ni(II) and Cu(II) Complexes with N-(Benzylcarbamothioyl) Benzamide as Corrosion Inhibitors for Mild Steel in 1M HCl, American Institute of Physics, 2(9): 36-89.

38. Abbas AS, Zainab AH (2016) Spectroscopic Studies and Thermal Analysis of New Azo Dyes Ligands and their Complexes with some Transition of Metal Ions, Baghdad Science Journal, 13(3): 511-523.

39. Ammar J, Mohammed H (2019) Synthesis, Thermal Study and Biological Activity of Cobalt (II)and Copper (II) Mixed Ligand Complexes Using (N-4-Methoxy Phenyl) Amino Phenyl Acetonitrile and Histidine Ligands, J. Pharm. Sci. & Res., 11(1): 155-158.

40. Sagar VS, Raju MP, Ram SD (2013) Corrosion Inhibition of mild steel by using mixed ligand metal complexes, Int. J. Chem. Sci., 11(1): 503-517.

41. Elsayed TH, Esam AG (2015) Conductometric, Spectrophotometric and In vivo Investigation of the Interaction of Ca(II) Ion with Oxytetracycline Hydrochloride,International Journal of Pharma Medicine and Biological Sciences, 4(3): 12-23.

42. Gharda N, Galai M, Saqalli L (2017) Synthesis, Structural Properties and Complex Corrosion Inhibition Cu (II) With Amino Acid (DL-a-Alanine), oriental journal of chemistry, 33(4): 1665-1676.